Effect of ZnS Nanofiller and Temperature on Mechanical Properties of Poly(methyl methacrylate)

Sonalika Agarwal, Dinesh Patidar, N. S. Saxena

Semi-Conductor & Polymer Science Laboratory, University of Rajasthan, Jaipur 302055, India

Received 18 February 2011; accepted 27 April 2011
DOI 10.1002/app.34800
Published online 24 August 2011 in Wiley Online Library (wileyonlinelibrary.com).

ABSTRACT: This article deals with the study of some mechanical properties of ZnS/poly(methyl methacrylate) nanocomposites prepared by solution casting method. The obtained ZnS/PMMA nanocomposites have ZnS nanoparticles in (0, 2, 4, 6, and 8) wt % and characterized through X-ray diffraction (XRD), transmission electron microscope (TEM), scanning electron microscope (SEM), and Fourier transform infrared (FTIR) spectroscopy measurements. Mechanical properties of ZnS/PMMA nanocomposites have been determined at different temperatures (30°C, 50°C, 70°C, and 90°C) through their stress–strain behavior using dynamic mechanical analyzer (DMA). The properties have been found to increase upto 6 wt % of ZnS nanoparticles and then decrease for 8 wt % of ZnS nanoparticles. A theoretical model has also been employed to predict the strain softening and strain hardening of the material. © 2011 Wiley Periodicals, Inc. J Appl Polym Sci 123: 2431–2438, 2012

Key words: mechanical properties; nanocomposites; strength; interfacial adhesion

INTRODUCTION

Poly(methyl methacrylate) (PMMA) has been extensively employed because it is easily available and presents good environmental stability, possesses light-weight and bears low cost. Besides this, it is an important transparent thermoplastic material[1,2] that finds applications in light emitting devices, batteries, optics, electromagnetic shielding, glazing, air-crafting and many applications.[3–10] However, their poor mechanical strength limits their range of applications. To improve their mechanical and thermal stability, the nanofillers are incorporated into polymer. The introduction of filler in a host matrix gives desirable material properties, which have not been achieved by matrix phase alone. Using this approach, polymer's properties can be improved while maintaining its light-weight and ductile nature. Recently various nanoscale fillers, including silica, alumina, zinc oxide, titanium oxide, zirconia, carbon nanotubes (CNT) etc.[11–15] have been reported to enhance mechanical and thermal properties of polymers, such as toughness, stiffness, and heat resistance. Etienne et al.[16] have investigated the effect of incorporation of modified silica nanoparticles on the mechanical and thermal properties of PMMA. Their results showed the improvement of thermal stability and mechanical properties by incorporation of silica nanoparticles in PMMA matrix. Chatterjee[17] has studied the mechanical and thermal properties of PMMA using nano-TiO_2. It was found that thermal stability is improved due to heat inhibiting effects of the TiO_2 particles in the degradation stages of PMMA. Luo et al.[18] have discussed the mechanical research of CNT/PMMA composite films. They found that the mechanical properties of the composite films have improved with the increased concentration of CNTs. Hu et al.[19] have studied the surface mechanical properties of transparent poly (methyl metacryalte)/zirconia nanocomposites prepared by *in situ* bulk polymerization. It was observed that at low ZrO_2 content, the mechanical properties were improved due to the formation of cross-linking structure. A remarkable improvement of hardness and scratch resistance of PMMA were achieved when 15 wt % of ZrO_2 content was embedded. Viratyaporn et al.[20] have discussed the effect of nanoparticles (Al_2O_3 and ZnO) on the thermal stability of PMMA nanocomposites prepared by *in situ* bulk polymerization. The results indicated that addition of nanoparticles affects degradation mechanism and consequently improves the thermal stability of PMMA. The reduction of polymer chain mobility and the tendency of nanoparticles to eliminate free radicals are the principal effects responsible for these enhancements.

From the literature survey, it is observed that effect of ZnS nanofiller on mechanical properties of PMMA have been studied very scantly because ZnS has been known as one of the most promising

Correspondence to: S. Agarwal (sonalika.spsl@gmail.com) or N. S. Saxena (n_s_saxena@rediffmail.com).

photo-sensitive material owing to its unique photochemical properties. The nanocomposites of ZnS can provide the possibility to obtain combinations of functionalities such as thermal stability with good mechanical and optical properties. In view of this, in this article, our main objective was to study the mechanical properties such as Young Modulus, tensile strength, yield strength, and fracture energy of ZnS/PMMA nanocomposites with temperature to produce mechanically viable composites which could be effectively used in optoelectronic devices employed in optical communication. Besides this, a constitutive model has also been applied to ZnS/PMMA nanocomposites to predict both strain hardening and strain softening characteristics of polymer nanocomposites.

EXPERIMENTAL

Preparation of polymer nanocomposites

ZnS nanoparticles were synthesized following procedures published elsewhere.[21] The fine powder of ZnS nanoparticles has now been used to prepare ZnS/PMMA nanocomposite by solution casting method. In this method, firstly PMMA has been dissolved in tetrahydrofurane (THF) solution by magnetic stirrer for 2 h and then ZnS nanoparticles with different weight percent (0, 2, 4, 6, and 8) have been dispersed into THF solution containing PMMA. The obtained solutions have been agitated by ultrasonicator to get the uniform distribution of ZnS nanoparticles in the solution. These solutions have been poured in the petri-dishes to obtain the ZnS/PMMA nanocomposite films. After 2 days, the nanocomposite films have been taken out from the petri-dishes and dried in vacuum of 10^{-2} torr for 6 h to remove the solvent. The thickness of prepared samples is 0.1–0.2 mm.

Structural characterization

In this study, X-ray diffraction (XRD) has been used to confirm the amorphous and crystalline phases present in the material. Besides this, it also provides an estimate of the approximate average size of the nanoparticles. The XRD spectra of the nanocomposites were recorded using Bragg-Brentanno geometry on a Panalytical X'pert Pro diffractometer with a Cu Kα radiation source ($\lambda = 1.5406$ Å). The X-ray tube was operated at 45 kV and 40 mA.

To study the structure of thin films in terms of dislocation and size of the nanoparticles in the nanocomposites transmission electron microscopy (TEM) measurements have been employed. The TEM measurements of nanocomposites were performed on TECNAI G2 30 U-TWIN system operating at an accelerating voltage of 300 kV. The samples for TEM measurement were prepared by dissolving ZnS/PMMA nanocomposite films in THF solvent using ultrasonicator. A drop of prepared solution was placed on the carbon coated copper grid and solvent removed by evaporation at room temperature.

The surface morphology of the ZnS/PMMA nanocomposites was studied using scanning electron microscopy (SEM) Quanta Fe-200 model. The sample to be examined was placed on a specimen stub and then gold was placed on the upper surface of the sample to make it conductive. Conductive silver paste was used to attach the specimen to the sample holder.

The Fourier transform infrared (FTIR) spectroscopy measurements of ZnS/PMMA nanocomposites were recorded in the wave number region 4000–400 cm^{-1}, using model IR Affinity-1, Shimadzu spectrophotometer. The accuracy of the measurement is ± 4 cm^{-1} in 4000–2000 cm^{-1} region and ± 2 cm^{-1} in 2000–400 cm^{-1} region.

Dynamic mechanical analyzer

The mechanical properties of the nanocomposites have been measured by Tritec 2000 dynamic mechanical analyzer (DMA). The details about DMA have been discussed elsewhere.[22–23] For such measurements, samples were cut to be between 2–3 mm in width and 8.05 mm in length. The mechanical properties such as Young Modulus, tensile strength, yield strength, and fracture energy determined although stress–strain measurements were performed at room temperature (30°C) as well as at elevated temperatures (50, 70, and 90°C) with load rate 0.1N/min in tension mode. The applied force is 10N.

RESULTS AND DISCUSSION

Morphology

The XRD patterns of pure PMMA and ZnS/PMMA nanocomposites are also shown in Figure 1. This figure shows one broad hump and three broad peaks in the XRD pattern of the nanocomposites. The first broad hump at lower diffraction angle around (10–20°), shows the amorphous nature of PMMA. The other three peaks at angles 28.8°, 47.8°, and 56.6° corresponding to (101), (103), and (004) planes respectively indicate the hexagonal phase of ZnS nanoparticles.[21] The XRD data is refined removing the broadening due to instrument and non uniform strain present in the lattice. The broadening of XRD peak (β_o) is observed due to small particle (β_d), instrumental (β_i) and strain induced (β_ε) broadening in the materials and it is given by $\beta_o = \beta_d + \beta_i + \beta_\varepsilon$.

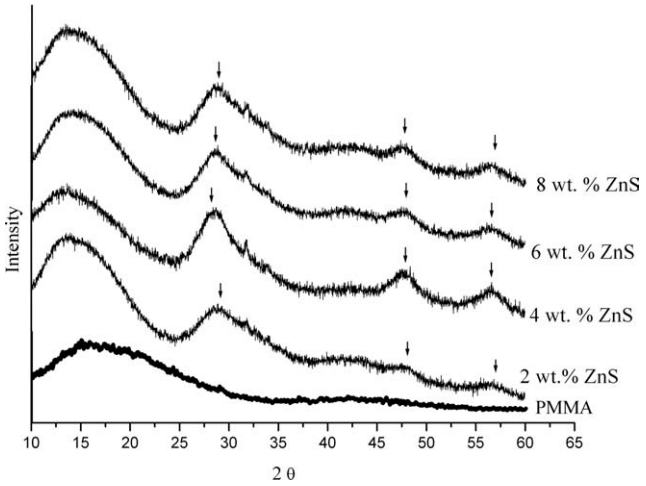

Figure 1 XRD patterns of PMMA and ZnS/PMMA nanocomposites.

The exact particle size of material has been determined by removing the peak broadening produced by instrumental and strain induced broadening. The instrumental broadening β_i is directly determined through the system using XRD of Si as standard material and removed from the observed peak broadening so that the instrumental corrected broadening ($\beta_c = \beta_o - \beta_i$) is observed. The line broadening β_d originating from the small particle size follows Scherrer equation[24] $\beta_d = k\lambda/d \cos\theta$, where k is the shape factor, λ is the X-ray wavelength, θ is the Bragg angle, and d is the effective particle size. The strain induced broadening β_ε is given by the Wilson formula as $\beta_\varepsilon = 4\varepsilon\tan\theta$, where ε is the root mean square value of the micro strain. Assuming that the particle size and strain contributions to line broadening are independent of each other so that the observed line breadth is simply the sum of the two terms, i.e., $\beta_c = \beta_d + \beta_\varepsilon = [k\lambda/d \cos\theta] + [4\varepsilon\tan\theta]$ or $\beta_c \cos\theta = k\lambda/d + 4\varepsilon\sin\theta$. This equation is the Williamson-Hall equation. Now Plot the curve between $\beta_c \cos\theta$ and $4\sin\theta$ and the micro strain ε is calculated from the slope of the line of the curve. This value of ε is again used in Williamson-Hall equation for determination of average particle size (d). The average particle size of ZnS nanoparticles is calculated to be 3 nm.

Figure 2(a–d) shows the TEM micrographs of ZnS/PMMA nanocomposites for 2, 4, 6, and 8 wt % of ZnS nanoparticles, respectively. The average particle size of ZnS nanoparticles is approximately 5 nm. The particle size obtained from XRD and TEM differs slightly from each other. This slight difference in particle size estimation using XRD and TEM is due to the intrinsic twining and dislocations present in the lattice of sample. The TEM images for 2 and 4 wt % of ZnS nanoparticles indicate that the particles are well dispersed in PMMA whereas small agglomeration is found for 6 wt % and the agglomeration is enhanced for 8 wt % of ZnS nanoparticles.

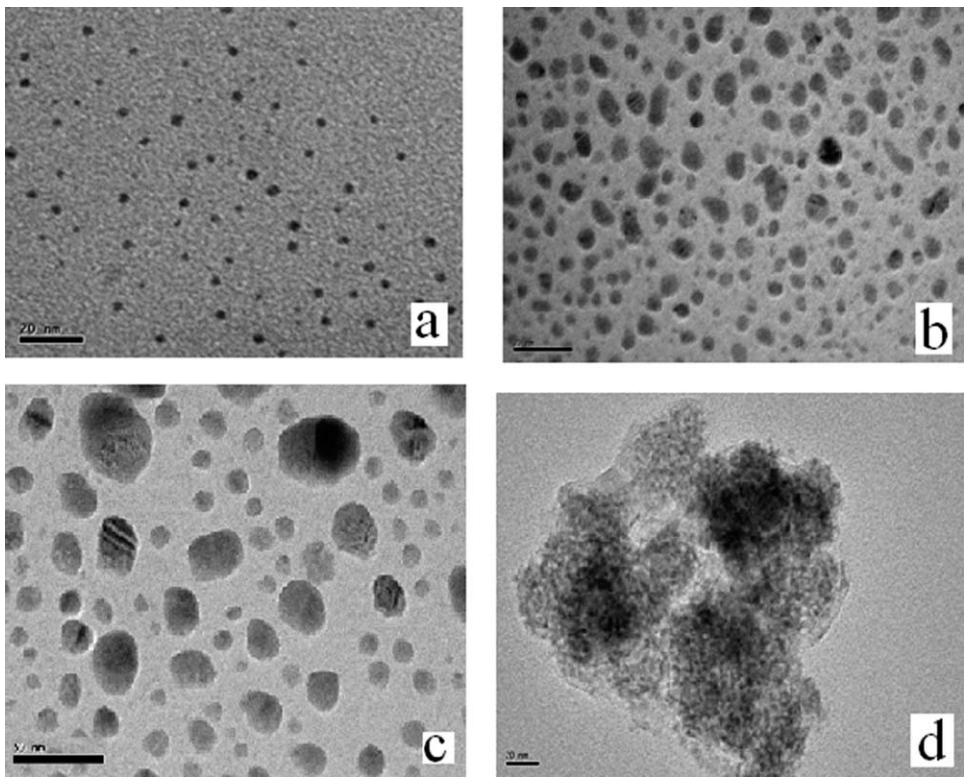

Figure 2 TEM micrographs of (a) 2 wt % ZnS/ PMMA, (b) 4 wt % ZnS/ PMMA, (c) 6 wt % ZnS/ PMMA, and (d) 8 wt % ZnS/ PMMA.

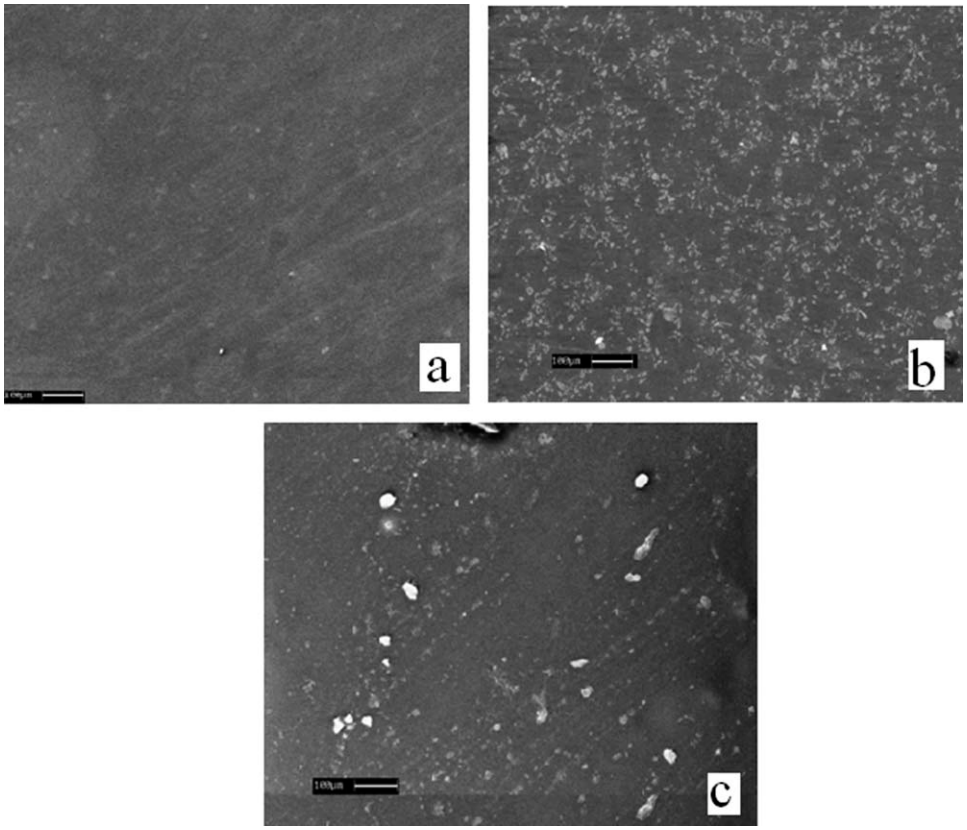

Figure 3 SEM micrographs of (a) Pure PMMA, (b) 6 wt % ZnS/PMMA, and (c) 8 wt % ZnS/PMMA.

Figure 3(a–c) shows the SEM micrographs of pure PMMA and ZnS dispersed PMMA nanocomposites. From the figure, it is observed that dispersed ZnS filler particles create considerable change in morphology of the pure PMMA film. In ZnS/PMMA nanocomposites, ZnS nanoparticles upto 6 wt % have almost uniform dispersion (with very small agglomeration) whereas particles are agglomerated at higher weight percentage (8 wt %) of ZnS nanoparticles (Fig. 3). The figure also demonstrates that interaction between PMMA matrix and ZnS nanoparticles increases with the increase of ZnS content into PMMA upto 6 wt %, whereas for 8 wt % of ZnS nanoparticles into PMMA matrix, interaction between nanoparticles is larger as compared with polymer–particle interaction, which causes the agglomeration of ZnS nanoparticles.

Figure 4 shows the FTIR spectra of the pure PMMA and ZnS/PMMA nanocomposites. The characteristic peaks of the stretching vibration bands of the C=O, C=C and C—H bonds in the PMMA segment have been observed at 1730, 1960, and 760, 2820–3050 cm^{-1}, respectively.[25] Besides these bands, the additional bands related to ZnS at 630 and 3440 cm^{-1} have been observed in the spectra of ZnS/PMMA nanocomposites.[26] Weak band at 630 cm^{-1} is also assigned to the stretching vibration of C-S group.[27] The presence of these bands indicates the chemical bonding between PMMA chains and ZnS nanoparticles.

Mechanical properties

Figures 5–8 show the stress–strain curves of ZnS/PMMA nanocomposites with different weight

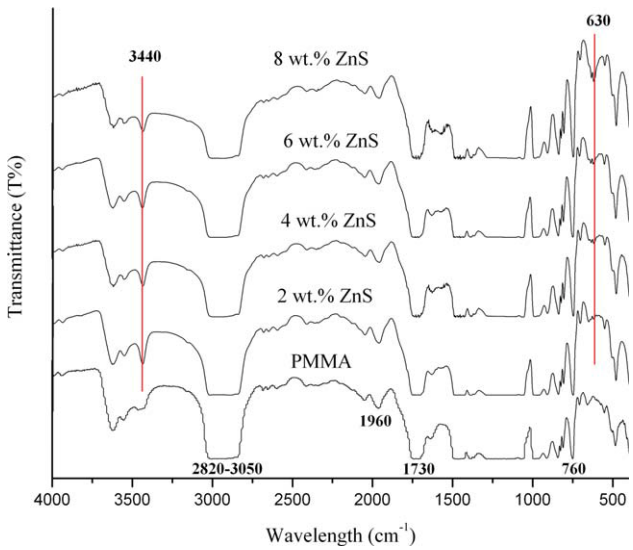

Figure 4 FTIR spectra of PMMA and ZnS/PMMA nanocomposites. [Color figure can be viewed in the online issue, which is available at wileyonlinelibrary.com.]

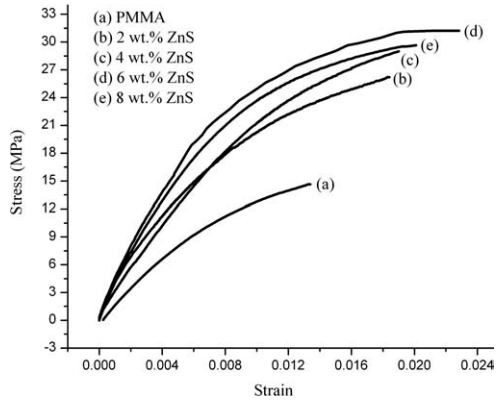

Figure 5 Stress–strain behavior for ZnS/PMMA nanocomposites at 30°C.

percent of ZnS nanoparticles at room (30°C) as well as at elevated (50°C, 70°C, and 90°C) temperatures. From Figure 5, it is observed that all ZnS/PMMA nanocomposites show no yield point and no break point at room temperature. This is due to the fact that in the given experiment the applied force of 10N is not sufficient (the limit of applied force in the used experiment is 10N) to produce any yield and break point. Hence, it is not possible to obtain the value of tensile strength, yield strength and fracture energy at room temperature.

All the mechanical properties such as Young's modulus, tensile strength, yield strength, and fracture energy obtained from the stress–strain relation have been summarized in Table I. Young's modulus is determined from the elastic linear region of the stress–strain curves whereas tensile strength is the maximum stress at break point. The total area under the stress–strain curve is defined the fracture energy. This fracture energy is related to the toughness of polymer. It is noticed from the Table I that all these properties show higher value for ZnS/PMMA nanocomposites than that of pure PMMA. The results obtained from this study are explained on the basis of interaction between ZnS nanoparticles and polymer matrix. The increase in the mechanical properties is attributed to the interaction between nanoparticles and polymer matrix.[28,29] The interaction between PMMA and ZnS is identified through C—S (630 cm^{-1}) bonding which is shown in FTIR spectra (Fig. 4). This is a weak interaction (Van der Waals interaction) between PMMA and ZnS nanoparticles. The nanoparticles have high surface area compared with the conventional fillers and have good interfacial adhesion with the polymer chains so that the mobility of polymer chains is restricted under loading, which increases Young's modulus.[30–33] Similarly, the increment in tensile strength and in yield

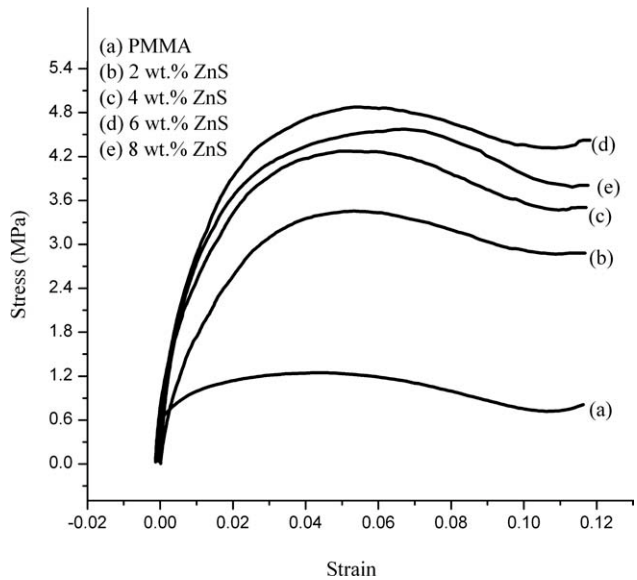

Figure 7 Stress–strain behavior for ZnS/PMMA nanocomposites at 70°C.

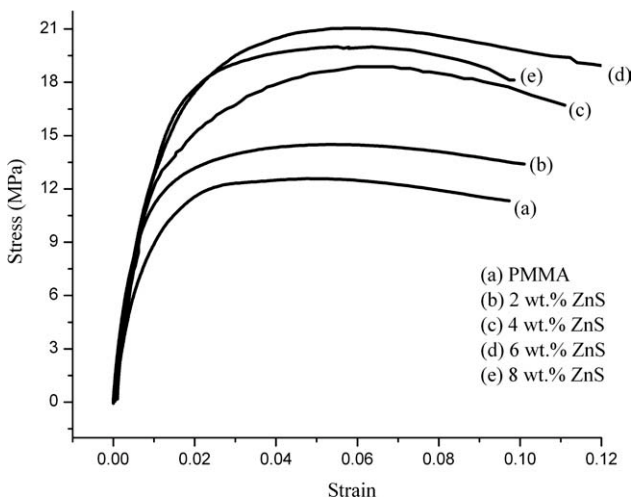

Figure 6 Stress–strain behavior for ZnS/PMMA nanocomposites at 50°C.

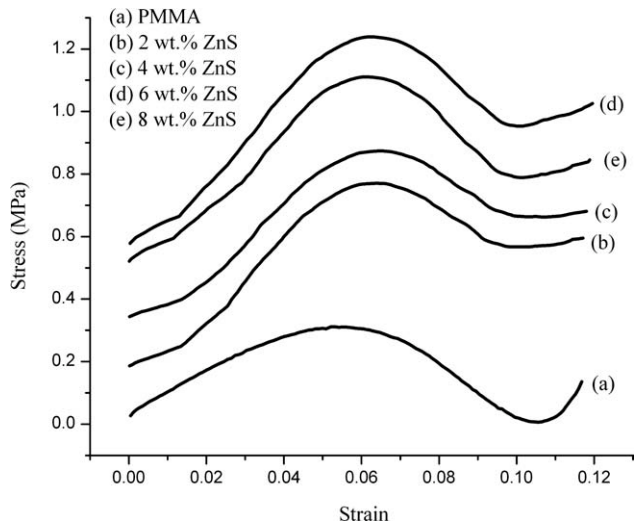

Figure 8 Stress–strain behavior for ZnS/PMMA nanocomposites at 90°C.

TABLE I
Mechanical Properties of ZnS/PMMA Nanocomposites

Sample	Temperature (°C)	Young's modulus (MPa)	Tensile strength (MPa)	Yield strength (MPa)	Fracture energy (10^{-3}J)
PMMA	30	1597	–	–	–
	50	1240	11.33	12.58	3.27
	70	58	0.81	1.24	0.26
	90	5	0.13	0.31	0.07
PMMA with 2 wt % ZnS	30	2220	–	–	–
	50	1361	13.40	14.50	3.78
	70	176.4	2.87	3.40	0.87
	90	11.11	0.60	0.78	0.20
PMMA with 4 wt % ZnS	30	2360	–	–	–
	50	1390	16.71	18.87	5.77
	70	256.6	3.50	4.19	1.17
	90	12.42	0.71	0.89	0.27
PMMA with 6 wt % ZnS	30	3330	–	–	–
	50	1452	18.90	21.04	7.67
	70	318.9	4.42	4.80	1.76
	90	14.5	1.12	1.26	0.31
PMMA with 8 wt % ZnS	30	2960	–	–	–
	50	1414	18.1	19.98	5.81
	70	280.1	3.80	4.48	1.41
	90	12.53	0.92	1.14	0.29

strength is attributed to the nano reinforcement of the fillers used, which facilitates efficient stress transfer to the filler.[34] The fracture energy also shows increasing behavior with the addition of nanoparticles up to 6 wt % at all temperatures. It is also observed from Table I that all mechanical properties decrease at 8 wt % (beyond 6 wt %) of ZnS nanoparticles in PMMA. The same behavior is observed for glass transition temperature (T_g) of ZnS/PMMA nanocomposites and thermal conductivity measurements of CdS/PMMA nanocomposites with filler concentration.[21,35] The decrease in the mechanical properties is caused due to the change in dispersion of nanoparticles from uniform to agglomeration. Due to the agglomeration of the nanoparticles, the particle–particle interaction is predominant over the filler–polymer interaction. Also agglomerated particles act as defects.[36,37] As a result, the decrease in mechanical properties is observed.

From Figures 5–8 and Table I, it is observed that Young's modulus and tensile strength are maximum for all composites at room temperature. Young's modulus and tensile strength decrease with the increase in temperature. This behavior of stress–strain curves can be explained on the basis of molecular motion of polymer chains. At low temperature, the structure is rigid and compact therefore the molecular motion in polymer is small due to the low kinetic energy of molecules, which ultimately leads to high Young modulus and tensile strength. As the temperature is increased to 50°C, the kinetic energy of molecules increases, which further increases the molecular motion resulting in an increase in the loosely bound structure, thereby decreasing the above-mentioned properties. On further increasing the temperature, i.e., at temperature (70°C and 90°C) in the vicinity of glass transition temperature, the molecular motion is further enhanced for viscous flow and the samples becomes soft and rubbery. The values of glass transition temperature[21] with ZnS concentration is shown in Table II. This consequently decreases the Young's modulus and tensile strength to a great extent and very low values of Young's modulus and tensile strength are obtained. Similar trend is followed by fracture energy, which is high at 50°C and decreases drastically with increasing the temperature (70°C and 90°C). The tensile strength increases 361%, 446%, 761%, and 607% for 2, 4, 6, and 8 wt % of ZnS nanocomposites as compared with pure PMMA near the glass transition temperature (90°C), respectively. The behavior of fracture energy at 90°C shows 185%, 285%, 342%, and 314% increment with ZnS concentration 2, 4, 6, and 8 wt % as compared with pure PMMA, respectively.

To describe the temperature dependent tensile behavior of ZnS/PMMA nanocomposite, as obtained

TABLE II
Glass Transition Temperature (T_g) Values for the ZnS/PMMA Nanocomposites

Samples	T_g (°C)
PMMA	82.1
PMMA with 2 wt % ZnS	89.6
PMMA with 4 wt % ZnS	91.4
PMMA with 6 wt % ZnS	99
PMMA with 8 wt % ZnS	93.6

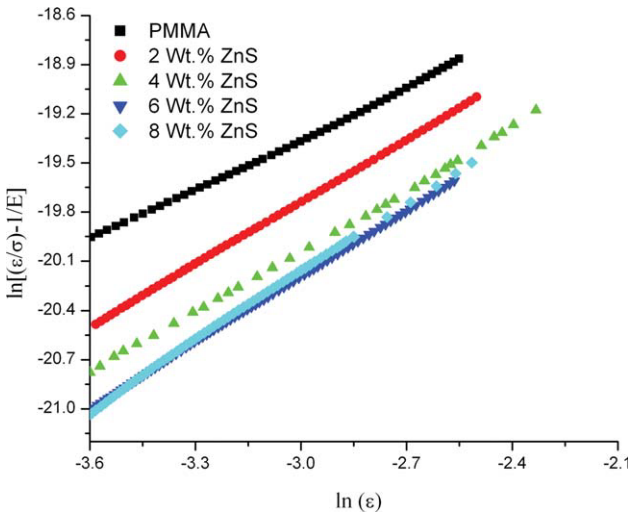

Figure 9 Variation of ln $(\varepsilon/\sigma - 1/E)$ with ln ε for ZnS/PMMA polymer nanocomposites at 50°C. [Color figure can be viewed in the online issue, which is available at wileyonlinelibrary.com.]

through experimental results, a three parameter constitutive model proposed by Zhou et. al.[38] has been employed. In this model, the total stress depends on the three parameters (elastic modulus, strain exponent, and compliance factor) and is given by the following relation:

$$\sigma = E(\acute{\varepsilon}, T)\varepsilon/\{1 + E(\acute{\varepsilon}, T)\beta(\acute{\varepsilon}, T)\varepsilon^m\} \quad (1)$$

Equation (1) is rewritten as follows

$$\varepsilon/\sigma - 1/E = \beta(\acute{\varepsilon}, T)\varepsilon^m \quad (2)$$

Taking log on both sides, of eq. (2) transforms into

$$\ln\,(\varepsilon/\sigma - 1/E) = \ln\,\beta + m\,\ln\,\varepsilon \quad (3)$$

where, E is elastic modulus of the material, which is a function of both strain rate ($\acute{\varepsilon}$) and temperature (T) and ε is total strain composed of elastic and inelastic part, β is a compliance factor which controls the flow stress level of the material and m is a strain exponent. The polymer behaves as a strain-hardening material when strain exponent $m < 1$ and as a strain-softening material when $m > 1$. When $m = 1$, the slope of the stress–strain curve becomes zero and the polymer is strain neutral, i.e., it is neither strain-hardening, nor strain-softening. Thus eq. (1) can be used to describe either a strain-hardening, strain-softening, or strain-neutral behavior with the help of value of m.

Figure 9 shows the variation of ln $(\varepsilon/\sigma - 1/E)$ with ln ε for ZnS/PMMA nanocomposites at temperature 50°C at constant strain rate as a representative case. Similar trend is observed at other temperatures. The data is fitted to straight line and the slope of this straight line gives the value of m and ln β. It can be observed that these plots are linear for all nanocomposites and are nearly parallel to each other, which means that material has the same strain exponent at different test conditions. The values of m and β are given in Table III. From Table III, it is observed that the values of m are <1 at 30°C temperature while it is >1 for 50°C, 70°C, and 90°C temperatures for all composites. Results indicate that m is almost independent of concentration of ZnS content in PMMA matrix and depends only on the temperature. This suggests the fact that at low temperature the material is rigid whereas at high temperature, it turns into softer material. This is also indicated from the mechanical properties. From Table III, it can also be noticed that the compliance factor (β) increases with the increase of temperature. This shows that stress flow level increases with increase of β, i.e., by increasing temperature.

CONCLUSIONS

Mechanical properties of ZnS/PMMA nanocomposites improve with the increase of concentration of ZnS nanoparticles in PMMA upto 6 wt % due to reasonably good interaction between ZnS nanoparticles and PMMA matrix and a notable decrease in mechanical properties beyond 6 wt % is due to the change in the dispersion of ZnS particles in polymer matrix from uniform to agglomeration. Mechanical properties of nanocomposites also show decreasing behavior with the increase of temperature due to the softening of

TABLE III
Constitutive Parameters of ZnS/PMMA Nanocomposites

	Temperature (°C)	PMMA	PMMA with 2 wt % ZnS	PMMA with 4 wt % ZnS	PMMA with 6 wt % ZnS	PMMA with 8 wt % ZnS
m	30	0.56	0.52	0.53	0.53	0.55
	50	1.03	1.26	1.27	1.36	1.40
	70	1.44	1.50	1.47	1.44	1.40
	90	1.87	1.82	1.91	1.71	1.69
β (1/MPa)	30	0.009	0.008	0.008	0.008	0.009
	50	0.087	0.120	0.087	0.101	0.121
	70	0.591	0.831	0.674	0.580	0.499
	90	0.658	0.583	0.580	0.189	0.183

material. The values of m and β indicate that all nanocomposites show the strain hardening behavior at room temperature, whereas show strain softening behavior at higher temperature and also show the increase in stress flow with increase of temperature.

Authors are thankful to Council of Scientific and Industrial Research (CSIR), New Delhi for providing financial assistance through Emeritus Scientist scheme during the course of this work. Thanks for providing facility of TEM at USIC, Delhi University, Delhi. One of us (Sonalika Agrawal) is also thankful to Dr. Deepika, Ms. Manasvi Dixit, and Mr. Mahesh Baboo for their help in various ways.

References

1. Arshad, M.; Masud, K.; Arif, M.; Rehman, S.; Arif, M.; Zaidi, J. H.; Chohan, Z. H.; Saeed, A.; Qureshi, A. H. J Therm Anal Calorim 2009, 96, 873.
2. Nemec, J. W.; Bauer, W. I., Jr. In Encyclopedia of Polymer Science and Engineering; Mark, H. F.; Bikales, N. M.; Overberger, C. G.; Marges, G., Eds.; New York: Wiley Interscience, 1985; Vol. 1,p 211.
3. Ishigure, Y.; Iijima, S.; Ito, H.; Ota, T.; Unuma, H.; Takahashi, M.; Hikichi, Y.; Suzuki, H. J Mater Sci 1999, 34, 2979.
4. Sumita, M.; Shizuma, T.; Miyasaka, K.; Ishikawa, K. J Macromol Sci Phys B 1983, 22, 601.
5. Sumita, M.; Shizuma, T.; Miyasaka, K.; Ishikawa, K. J Mater Sci 1983, 18, 1758.
6. Ray, S. S.; Biswas, M. Synth Met 2000, 108, 231.
7. Quivy, A.; Deltour, R.; Jansen, A. G. M.; Wyder, P. Phys Rev B: Condens Matter 1989, 39, 1025.
8. Harper, C. A. Modern Plastics Handbook; New York: McGraw-Hill, 2000.
9. Rajkumar, T.; Vijayakumar, C. T.; Sivasamy, P.; Sreedhar, B.; Wilkie, C. A. J Therm Anal Calorim 2010, 100, 651.
10. Wang, H.; Xu, P.; Zlong, W.; Shen, L.; Du, Q. Polym Degrad Stab 2005, 87, 319.
11. Ash, B. J.; Schadlen, L. S.; Siegel, R. W. Mater Lett 2002, 55, 83.
12. Sun, D.; Miyatake, N.; Sue, H. J. Nanotechnology 2007, 18, 215606.
13. Lee, L. H.; Chen, W. C. Chem Mater 2001, 13, 1137.
14. Yang, F.; Nelson, G. L. J Appl Polym Sci 2004, 91, 3844.
15. Guthy, C.; Du, F.; Brand, S.; Winey, K. I.; Fischer, J. E. J Heat Transfer 2007, 129, 1096.
16. Etienne, S.; Becker, C.; Ruch, D.; Grignard, B.; Cartigny, G.; Detrembleur, C.; Calberg, C.; Jerome, R. J Therm Anal Calorim 2007, 87, 101.
17. Chatterjee, A. J Appl Polym Sci 2010, 118, 2890.
18. Luo, J. T.; Wen, H. C.; Wu, W. F.; Chou, C. P. Polym Compos 2008, 29, 1285.
19. Hu, Y.; Zhou, S.; Wu, L. Polymer 2009, 50, 3609.
20. Viratyaporn, W.; Lehman, R. L. J Therm Anal Calorim 2011,103,
21. Agrawal, S.; Patidar, D.; Saxena, N. S. Phase Transit 2011, DOI: 10.1080/01411594.2011.563152.
22. Menard, K. P. Dynamic Mechanical Analysis: A practical introduction; CRC presses LLC: Boca Raton, Florida,1999.
23. Agrawal, S.; Patidar, D.; Dixit, M.; Sharma, K.; Saxena, N. S. AIP Proceeding 2010, 1249, 79.
24. Guinier, A. X-ray Diffraction; W. A. Freeman and Co., San Francisco, CA, 1963.
25. Sharma, Y. R. Elementary organic Spectroscopy; S. Chand Company Ltd.: Ram Nagar, New Delhi, India,2003.
26. Park, K.; Yu, H. J.; Chung, W. K.; Kim, B. J.; Kim, S. H. J Mater Sci 2009, 44, 4315.
27. Sajinovic, D.; Saponjic, Z. V.; Cvjeticanin, N.; Marinovic-Cincovic, M.; Nedeljkovic, J. M. Chem Phys Lett 2000, 329, 168.
28. Maji, P. K.; Guchhait, P. K.; Bhowmick, A. K. J Mater Sci 2009, 44, 5861.
29. Wei, C. L.; Zhang, M. Q.; Rong, M. Z.; Friedrich, K. Comp Sci Technol 2002, 62, 1327.
30. Yilmazer, U.; Ozden, G. Polym Compos 2006, 27, 249.
31. Schick, C.; Wurm, A.; Mohamed, A. Colloid Polym Sci 2001, 279, 800.
32. Maiti, M.; Bhowmick, A. K. Polym Eng Sci 2007, 47, 1777.
33. Liu, X.; Wu, Q. Polymer 2001, 42, 10013.
34. LeBaron, P. C.; Wang, Z.; Pinnavaia, T. J Appl Clay Sci 1999, 15, 11.
35. Saxena, N. S. J Polym Eng,2010, 30, 575.
36. Maiti, M.; Sadhu, S.; Bhowmick, A. K. J Appl Polym Sci 2006, 101, 603.
37. Nielsen, L. E. In Mechanical Properties of Polymers; Van Nostrand Reinhold: New York,1962.
38. Zhou, Y.; Mallick, P. K. Polym Eng Sci 2002, 42, 2461.